Sixteenth International Conference on
Geometry, Integrability and Quantization
June 6–11, 2014, Varna, Bulgaria
Ivaïlo M. Mladenov, Andrei Ludu
and Akira Yoshioka, Editors
Avangard Prima, Sofia 2015, pp 256–269
doi: 10.7546/giq-16-2015-256-269

THE MYLAR BALLOON: AN ALTERNATIVE DESCRIPTION

VLADIMIR I. PULOV, MARIANA TS. HADZHILAZOVA† and IVAÏLO M. MLADENOV†

Department of Physics, Technical University of Varna, Studentska Str. 1, 9010 Varna, Bulgaria

†*Institute of Biophysics and Biomedical Engineering, Bulgarian Academy of Sciences Acad. G. Bonchev Str., Block 21, 1113 Sofia, Bulgaria*

Abstract. Here we present a new parametrization of the Mylar balloon via the Weierstrassian functions which is used for the derivation of the basic geometrical characteristics of the balloon.

MSC: 49Q10, 53A05, 53A10
Keywords: Axisymmetric surfaces, balloons, Weierstrassian functions

1. The Mylar Balloon: Industrial and Geometrical

The Mylar® is a trademark of an extremely thin polyester film, which is flexible but superior inelastic – when folded it can neither stretch nor shrink. In geometry the term Mylar is the name coined by Paulsen [12] in order to designate a special surface of revolution. He called this surface "Mylar balloon", or shortly "Mylar", as it almost perfectly approaches the shape of a fully inflated balloon, made from two sewn together equal circular disks of Mylar® foil. Due to the great tensile strength of the foil, the resulting shape of the Mylar balloon is somewhat surprisingly not spherical in form and the surface area is not preserved – a fact extremely evidenced by the wrinkled area showing up along the sewn boundaries of the two disks. Such wrinkling and crimping are apparently observed for the commercially produced Mylar® balloons widely used for decoration purposes and kids toys.

The inflating of the Mylar balloon, as pictured above, clearly implies the following mathematical problem: *Find a surface of revolution, enclosing maximum volume, for a given directrice arclength.* Inflating of the balloon to the maximum and the non elasticity of the balloon's material are the physical conditions that presuppose this formulation. In order to pose the problem rigorously, we assume that the OZ-axis is the axis of revolution, and the curve in the XOZ-plane, $z = z(x)$, is taken to be the upper half of the right hand side of the balloon's directrice (see Fig. 1). Physically it is obvious that this curve smoothly decreases from its maximum height on the OZ-axis to a point on the OX-axis, i.e., $z(r) = 0$, for some positive r, and the derivative $\dot{z}(x)$ is negative for $0 < x < r$. Also, it is intuitively clear that the profile curve must cross the OX-axis perpendicularly. In order to meet these requirements we have to assume $\dot{z}(0) = 0$ and $\lim_{x\to r} \dot{z}(x) = -\infty$.

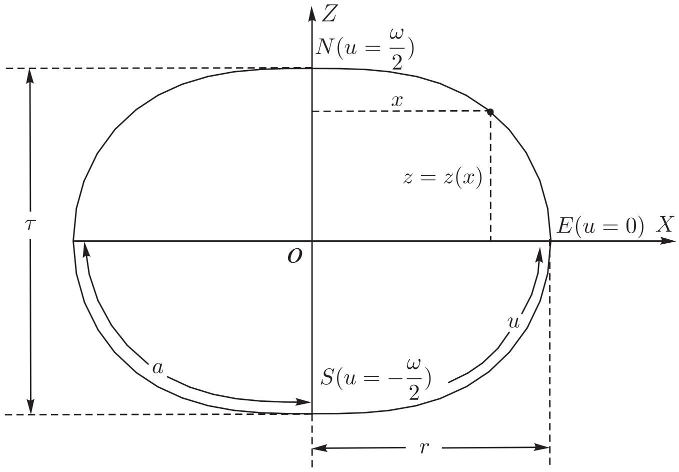

Figure 1. The profile curve of the Mylar balloon in the XOZ-plane, where a is the radius of the disks (deflated radius), r is the radius of the balloon (inflated radius) and τ is the thickness of the balloon.

Let a be the radius of the initially flat disks. On inflating of the balloon the disks start deforming, but the Mylar foil resists stretching, so that the length of their radii remains unchanged. Consequently, the arclength of the graph of $z(x)$ from $x = 0$ to $x = r$ remains fixed to a (Fig. 1). It follows from symmetry considerations that the bottom half of the Mylar balloon is obtained by reflection of its upper half part through the XOY-plane.

Now, we can state the problem in calculus of variations settings: *Find the profile curve* (*directrice*) *of the Mylar balloon*

$$z = z(x), \qquad z(r) = 0, \qquad \dot{z}(x) \le 0, \qquad 0 \le x \le r$$

by maximizing the volume

$$\mathcal{V} = 4\pi \int_0^r x z(x) \mathrm{d}x \tag{1}$$

subject to the constraint

$$\int_0^r \sqrt{1+\dot{z}^2(x)}\mathrm{d}x = a \tag{2}$$

and satisfying the transversality conditions

$$\dot{z}(0) = 0, \qquad \lim_{x\to r} \dot{z}(x) = -\infty.$$

Then, as it can be shown (cf also [8,9,11]), the constraint Euler-Lagrange equation takes the form

$$\frac{\mathrm{d}z}{\mathrm{d}x} = -\frac{x^2}{\sqrt{r^4 - x^4}}. \tag{3}$$

Thus far, we have introduced the problem of finding the shape of a fully inflated circular Mylar balloon using the same variational settings as they were given by Paulsen [12] in the first geometrical depiction of the balloon in 1994. Based on the equation (3) Paulsen succeeded in determining three characteristic measures of the balloon: the inflated radius r, the thickness $\tau = 2z(0)$ (see Fig. 1) and the volume $\mathcal{V}$. His results are expressed in terms of the Gamma function. In [11], solutions of the equation (3) were evaluated numerically via certain Maple subroutines, needed for obtaining the plotted picture of the balloon and expressing the three quantities r, τ and $\mathcal{V}$ in terms of the radius a of the deflated balloon. Explicit parametrizations of the Mylar via Jacobian elliptic functions and elliptic integrals have been derived in [7–9] and this leads to a deeper understanding of the geometry of the balloon.

In Section 2 we will present new alternative parametrization of the Mylar balloon by employing the Weierstrassian functions. In Section 3 we will derive systematically the basic geometrical characteristics of the balloon – the first and the second fundamental forms, the mean, the Gaussian and the principal curvatures. In Section 4 we proceed with determining the surface area, the volume and other measurable quantities of the balloon including the so called "crimping factor" and the moment of inertia of the "solid" Mylar, obtained again analytically with the help of the Weierstrassian functions. The graph of the balloon's profile (see Fig.1) and most of the lengthy and tedious analytical computations were accomplished with the help of the software package *Mathematica*®. The last section summarizes the obtained results and contains a comment about the fundamental in this setting lemniscate constant.

2. Parametrization via the Weierstrassian Functions

Looking for solutions of the variational problem posed in Section 1, we recast the related Euler-Lagrange equation (3) into the form of the following system of equations

$$\begin{aligned}\frac{\mathrm{d}x}{\mathrm{d}u} &= \sqrt{r^4 - x^4}\\ \frac{\mathrm{d}z}{\mathrm{d}u} &= x^2\end{aligned} \tag{4}$$

where $u \in \mathbb{R}$ is a new variable and the minus sign has been omitted which results in replacement of z by $-z$. Actually, the above system can be readily integrated in terms of the Weierstrassian functions and in this way we obtain the parametrization of the profile curve of the Mylar balloon (traced counterclockwise) in the form

$$(x(u), z(u)) = \left(r\,\frac{2\wp(u) - r^2}{2\wp(u) + r^2},\, 2\zeta(u) + \frac{2\wp'(u)}{2\wp(u) + r^2} \right), \quad u \in \left[-\frac{\omega}{2}, \frac{\omega}{2} \right] \tag{5}$$

where $\wp(u) \equiv \wp(u; -r^4, 0)$, $\wp'(u) \equiv \wp'(u; -r^4, 0)$ and $\zeta(u) \equiv \zeta(u; -r^4, 0)$ are respectively the Weierstrassian $\wp$-function $\wp(u)$, its derivative $\wp'(u)$ and the Weierstrassian zeta function $\zeta(u)$ built with the invariants [5, 13]

$$g_2 = -r^4, \qquad g_3 = 0 \tag{6}$$

and ω is the real-valued half-period of $\wp(u)$. The discriminant of $\wp(u)$

$$\Delta \equiv g_2^3 - 27 g_3^2 = -r^{12}$$

is obviously negative and this implies the relation

$$\omega = \omega_1 + \omega_2$$

in which ω_1 and ω_2 are the primitive (complex-valued in general) half-periods of $\wp(u)$. In view of the concrete values of the invariants g_2 and g_3 specified in (6) the Weierstrassian functions involved here are directly reducible to the so called pseudo-lemniscatic case with $g_2 = -1$, $g_3 = 0$ [1]. A pleasant consequence of this fact is the possibility to express the real half-period ω as a ratio of the lemniscate constant

$$\tilde{\omega} \approx 2.6220 \tag{7}$$

and the radius r of the balloon

$$\omega = \frac{\tilde{\omega}}{r} \cdot \tag{8}$$

Because the surface of Mylar is obtained by rotating the directrice (5) about the OZ-axis, the position vector of any point on this surface

$$\mathbf{x}(u, v) = (x(u, v), y(u, v), z(u, v))$$

is given by the formulas

$$
\begin{aligned}
x(u,v) &= r\,\frac{2\wp(u)-r^2}{2\wp(u)+r^2}\cos v, \qquad y(u,v) = r\,\frac{2\wp(u)-r^2}{2\wp(u)+r^2}\sin v \\
z(u,v) &= 2\zeta(u)+\frac{2\wp'(u)}{2\wp(u)+r^2}, \qquad u\in\left[-\frac{\omega}{2},\frac{\omega}{2}\right], \qquad v\in(0,2\pi].
\end{aligned}
\tag{9}
$$

Thus, the profile curve and the surface of Mylar are parameterized as specified by the equations (5) and (9) in terms of the Weierstrassian functions $\wp(u)$, $\wp'(u)$ and $\zeta(u)$. Note that the meridians (cf Fig. 1) are traced counterclockwise from S (the South Pole corresponding to $u=-\omega/2$), through the equator E (where $u=0$), to N (the North Pole where $u=\omega/2$).

Let us also mention some facts about the Weierstrassian functions. The Weierstrassian $\wp$-functionan $\wp(u)$ and its derivative $\wp'(u)$ are elliptic functions, hence doubly-periodic with a pair of complex-valued (primitive) periods $2\omega_1$ and $2\omega_2$, $\Im(\omega_2/\omega_1)\neq 0$. Related to $\wp(u)$ there are two additional functions – one of them is the so called Weierstrassian zeta function $\zeta(u)$ which appears above, and the other is the Weierstrassian sigma function $\sigma(u)$, defined by the equations

$$
\zeta'(u) = -\wp(u), \qquad \frac{\sigma'(u)}{\sigma(u)} = \zeta(u).
$$

Neither of them is doubly-periodic, but each one satisfies a quasi-periodicity condition

$$
\begin{aligned}
\zeta(u+2\omega_k) &= \zeta(u)+2\eta_k, \qquad \eta_k=\zeta(\omega_k), \qquad k=1,2 \\
\sigma(u+2\omega_k) &= -\,\mathrm{e}^{2\eta_k(u+\omega_k)}\sigma(u).
\end{aligned}
$$

The Weierstrassian $\wp(u)$ is even function, while $\wp'(u)$, $\zeta(u)$ and $\sigma(u)$ are odd functions.

Very useful for practical applications are the homogeneity relations that are valid for any $t\in\mathbb{C}^*$

$$
\begin{aligned}
\wp'(tu;\,t^{-4}g_2,t^{-6}g_3) &= t^{-3}\wp'(u;\,g_2,g_3) \\
\wp(tu;\,t^{-4}g_2,t^{-6}g_3) &= t^{-2}\wp(u;\,g_2,g_3) \\
\zeta(tu;\,t^{-4}g_2,t^{-6}g_3) &= t^{-1}\zeta(u;\,g_2,g_3) \\
\sigma(tu;\,t^{-4}g_2,t^{-6}g_3) &= t\sigma(u;\,g_2,g_3).
\end{aligned}
\tag{10}
$$

They allow us, by taking in particular $t=r$, to reduce our considerations to the pseudo-lemniscatic case. For $\wp(u)$ we have

$$
\wp(u;\,-r^4,0) = r^2\wp(ru;\,-1,0)
$$

thus discovering the expression (8) for the real half-period of $\wp(u)$ on knowing that the real half-period of the pseudo-lemniscatic $\wp$ is actually the lemniscate constant $\tilde{\omega}$. Similar reductions hold for the functions $\wp'(u)$, $\zeta(u)$ and $\sigma(u)$. In the next section, when we calculate certain values of the Weierstrassian functions, we will avail from the homogeneity relations again.

3. Geometry of the Mylar Balloon

We turn now to the geometry of the Mylar balloon, starting from the basic concepts of the differential geometry of surfaces – the first I and the second II fundamental forms [10]

$$I = E\mathrm{d}u^2 + 2F\mathrm{d}u\mathrm{d}v + G\mathrm{d}v^2, \qquad II = L\mathrm{d}u^2 + 2M\mathrm{d}u\mathrm{d}v + N\mathrm{d}v^2$$

with the coefficients, defined by

$$\begin{aligned} E &= \mathbf{x}_u \cdot \mathbf{x}_u, \qquad & F &= \mathbf{x}_u \cdot \mathbf{x}_v, \qquad & G &= \mathbf{x}_v \cdot \mathbf{x}_v \\ L &= \mathbf{x}_{uu} \cdot \mathbf{n}, \qquad & M &= \mathbf{x}_{uv} \cdot \mathbf{n}, \qquad & N &= \mathbf{x}_{vv} \cdot \mathbf{n} \end{aligned}$$

where the sub-indices denote the respective partial derivatives ($\mathbf{x}_u = \partial \mathbf{x}/\partial u$, $\mathbf{x}_{uu} = \partial^2 \mathbf{x}/\partial u^2, \ldots$) and $\mathbf{n}$ is the unit normal vector to the surface

$$\mathbf{n} = \frac{\mathbf{x}_u \times \mathbf{x}_v}{|\mathbf{x}_u \times \mathbf{x}_v|}.$$

For the Mylar balloon we obtain

$$\begin{gathered} E = r^4, \qquad F = 0, \qquad G = r^2 \left(\frac{2\wp(u) - r^2}{2\wp(u) + r^2} \right)^2 \\ L = 2r^3 \left(\frac{2\wp(u) - r^2}{2\wp(u) + r^2} \right), \qquad M = 0, \qquad N = r \left(\frac{2\wp(u) - r^2}{2\wp(u) + r^2} \right)^3. \end{gathered} \tag{11}$$

The mean H and the Gaussian K curvatures of the surface are calculated using the well known classical formulas (cf [10])

$$H = \frac{EN + GL - 2FM}{2(EG - F^2)}, \qquad K = \frac{LN - M^2}{EG - F^2}$$

and in our case we find respectively

$$H = \frac{3}{2r} \left(\frac{2\wp(u) - r^2}{2\wp(u) + r^2} \right), \qquad K = \frac{2}{r^2} \left(\frac{2\wp(u) - r^2}{2\wp(u) + r^2} \right)^2. \tag{12}$$

Two other characteristic curvatures, the so called meridional k_μ and parallel k_π principal curvatures are connected with H and K through the equations $H =$

$(k_\mu + k_\pi)/2$ and $K = k_\mu k_\pi$, whereby

$$k_\mu = H + \sqrt{H^2 - K}, \qquad k_\pi = H - \sqrt{H^2 - K}.$$

For the Mylar we compute directly

$$k_\mu = \frac{2}{r}\left(\frac{2\wp(u) - r^2}{2\wp(u) + r^2}\right), \qquad k_\pi = \frac{1}{r}\left(\frac{2\wp(u) - r^2}{2\wp(u) + r^2}\right). \tag{13}$$

Let us notice that the principal curvatures are related by the equation

$$k_\mu = 2k_\pi$$

which is satisfied identically everywhere on the balloon surface $\mathcal{S}$. Among other things this means that our surface is a representative of the so called Weingarten class of surfaces. Being in this class, it has been proven that the above relation defines uniquely $\mathcal{S}$ (cf [8]) and that the solution of another geometric equation

$$(\nu^3)_{uu} + 6\nu = 0, \qquad \nu = \nu(u) \tag{14}$$

can be used for its generation as well (see [3]).

Looking at (5) and (13) one can conclude also that the curvature of the profile curve $k = k_\mu$ is related to its x-coordinate by the equation

$$k = \frac{2}{r^2}\,x. \tag{15}$$

The latter can be easily recognized in another setting as the equation behind the rectangular Euler elastica (see [4] and [2]).

4. Various Applications

After all these preliminaries we are going to determine the thickness τ, the surface area $\mathcal{A}(\mathcal{S})$, and the volume $\mathcal{V}$ of the Mylar balloon, as well as some other important geometrical and mechanical characteristics of the balloon. Before turning to details let us mention that from now on the differentiations with respect to u will be denoted by dots.

Our first task will be to establish how r and a are related to each other. Despite that the Mylar is fully determined by its radius r, yet it is instructive to know the ratio between r and the radius of the Mylar disks a, which means to find the ratio of the radius of the inflated and the radius of the deflated balloon. To this aim we make use of the constrained condition of Section 1 by calculating the arclength along the meridian of the Mylar starting from the equator and ending at N (North Pole), see Fig. 1

$$\int\limits_0^{\omega/2} \sqrt{\dot{x}^2(u) + \dot{z}^2(u)}\,\mathrm{d}u = r^2\int\limits_0^{\omega/2} \mathrm{d}u = \frac{\omega r^2}{2} = a. \tag{16}$$

In the above calculations use has been made of the fundamental differential relation satisfied by the Weierstrassian $\wp$-function [6, 13]

$$\dot{\wp}^2(u) = 4\wp^3(u) - g_2\wp(u) - g_3. \tag{17}$$

Combining the result in (16) with the already known relations (7) and (8) one immediately obtains the very useful formulas

$$a = \frac{\tilde{\omega} r}{2} \approx 1.3110\, r, \qquad r = \frac{2a}{\tilde{\omega}} \approx 0.7627\, a. \tag{18}$$

Other truly geometrical quantity is the thickness τ of the Mylar, as it is usually called the distance SN between the South and North Poles of the balloon (Fig. 1)

$$\tau = 2z(\omega/2) = \frac{\pi r}{\tilde{\omega}} = \frac{2\pi a}{\tilde{\omega}^2}\cdot \tag{19}$$

On the way of establishing the above result we have made use of the values of the Weierstrassian functions (cf [1])

$$\wp(\omega/2) = \frac{r^2}{2}, \qquad \dot{\wp}(\omega/2) = -r^3, \qquad \zeta(\omega/2) = \frac{\pi}{4\omega} + \frac{r}{2}\cdot \tag{20}$$

The relations (19) reveal the invariance of the ratio of the thickness τ versus the diameter $d = 2r$ of the inflated balloon

$$\frac{\tau}{d} = \frac{\pi}{2\tilde{\omega}} \approx 0.5990.$$

Our further considerations are based upon the derivation of explicit expressions for the quadratures

$$J_k = \int\limits_{-\omega/2}^{\omega/2} \frac{\mathrm{d}u}{(2\wp(u) + r^2)^k}, \qquad k = 1, 2, \ldots. \tag{21}$$

For example, in order to calculate the total surface area of the Mylar $\mathcal{A}(\mathcal{S})$ we need to know the first quadrature J_1 as in this case we have

$$\begin{aligned} \mathcal{A}(\mathcal{S}) &= \iint\limits_{\mathcal{S}} \mathrm{d}\mathcal{A} = \int\limits_0^{2\pi} \int\limits_{-\omega/2}^{\omega/2} \sqrt{EG - F^2}\mathrm{d}u\mathrm{d}v \\ &= 2\pi r^3 \int\limits_{-\omega/2}^{\omega/2} \frac{2\wp(u) - r^2}{2\wp(u) + r^2}\,\mathrm{d}u = 2\pi\omega r^3 - 4\pi r^5 \int\limits_{-\omega/2}^{\omega/2} \frac{\mathrm{d}u}{2\wp(u) + r^2}\cdot \end{aligned}$$

In order to obtain J_1 we make use of the integral formula [5]

$$\int \frac{\mathrm{d}u}{\wp(u) - \wp(\mathring{u})} = \frac{1}{\dot{\wp}(\mathring{u})}\left[2u\zeta(\mathring{u}) + \ln\frac{\sigma(\mathring{u} - u)}{\sigma(\mathring{u} + u)}\right] \tag{22}$$

where $\mathring{u}$ is a complex number defined by the equation

$$\wp(\mathring{u}) = -\frac{r^2}{2}\cdot \tag{23}$$

Based on the homogeneity relations (10), we observe that combining the values of $\wp$ in (20) and (23), the following chain of equalities holds

$$\wp(\mp \mathrm{i}\omega/2;\, -r^4, 0) = -\wp(\omega/2;\, -r^4, 0) = -\frac{r^2}{2} = \wp(\mathring{u};\, -r^4, 0)$$

in which by i is denoted the imaginary unit. Hence, we can conclude that

$$\mathring{u} = \mathring{u}_{\mp} = \mp\frac{\mathrm{i}\,\omega}{2}\cdot \tag{24}$$

Again on the base of (10), (20) and (24) and following a similar mode of reasoning we obtain also the relations

$$\dot{\wp}(\mathring{u}_{\mp}) = \pm \mathrm{i}\, r^3, \qquad \zeta(\mathring{u}_{\mp}) = \pm \mathrm{i}\left(\frac{\pi}{4\omega} + \frac{r}{2}\right). \tag{25}$$

For calculating the quadrature J_1, besides the formulas for $\wp(\mathring{u})$, $\dot{\wp}(\mathring{u})$ and $\zeta(\mathring{u})$, given by (23) and (25), we need to know the difference of the values of the logarithmic term in (22), calculated at the two extremal points $u = -\omega/2$ and $u = \omega/2$ of the integration interval. By making use of (24) and the homogeneity relation

$$\sigma(\mathrm{i}\,(\omega/2 + \mathrm{i}\,\omega/2);\, -r^4, 0) = \mathrm{i}\,\sigma(\omega/2 + \mathrm{i}\,\omega/2;\, -r^4, 0)$$

the sought difference is easily obtained in the form

$$2\ln\frac{\sigma(\mathring{u}_{\mp} - \omega/2)}{\sigma(\mathring{u}_{\mp} + \omega/2)} = \mp\,\mathrm{i}\,\pi.$$

With this result at hand we compute the quadrature

$$J_1 = \frac{2r\omega - \pi}{4r^3} \tag{26}$$

and thence deduce the surface area of the Mylar balloon

$$\mathcal{A}(\mathcal{S}) = \pi^2 r^2.$$

Our next concern are the area of the meridional section Σ, the volume $\mathcal{V}$ and the moment ot inertia $\mathcal{J}$ about the symmetry axis of the balloon considered as a rigid body of uniform mass density. Computation of all these quantities goes through the higher degree quadratures J_k, up to order $k = 6$. Fortunately for that purpose we have at our disposal the recursion formula [14]

$$\frac{\dot{\wp}(\omega/2)}{2^k\left[\wp(\omega/2)-\wp(\mathring{u})\right]^k}-\frac{\dot{\wp}(-\omega/2)}{2^k\left[\wp(-\omega/2)-\wp(\mathring{u})\right]^k}$$
$$=-2k\dot{\wp}^2(\mathring{u})J_{k+1}+(1-2k)\ddot{\wp}(\mathring{u})J_k+6(1-k)\wp(\mathring{u})J_{k-1}+\left(\frac{3}{2}-k\right)J_{k-2} \tag{27}$$

valid for $k=1,2,\ldots$. Applying (27) repeatedly as many times as needed, and making use of (17), (20), (23) and (26), we obtain

$$J_2=\frac{r^2\omega^2-\pi r\omega+\pi}{4r^6\omega},\quad J_3=\frac{2r^2\omega^2-(3\pi+2)r\omega+6\pi}{16r^8\omega}$$

$$J_4=\frac{2r^2\omega^2-(3\pi+6)r\omega+9\pi}{24r^{10}\omega},\quad J_5=\frac{32r^2\omega^2-(33\pi+120)r\omega+120\pi}{384r^{12}\omega}$$

$$J_6=\frac{60r^2\omega^2-5(9\pi+40)r\omega+156\pi}{640r^{14}\omega}\cdot$$

In this way we can compute the area of the meridional section of the Mylar balloon (see Fig. 2) by expanding the fourth integral below and then integrating and summing up the respective terms

$$\Sigma=4\int_0^{\omega/2}x\mathrm{d}z=2\int_{-\omega/2}^{\omega/2}x\mathrm{d}z=2\int_{-\omega/2}^{\omega/2}x^3(u)\mathrm{d}u=2r^3\int_{-\omega/2}^{\omega/2}\left(\frac{2\wp(u)-r^2}{2\wp(u)+r^2}\right)^3\mathrm{d}u$$
$$=4r^3\left(\frac{\omega}{2}-3r^2J_1+6r^4J_2-4r^6J_3\right)=2r^2. \tag{28}$$

This can be done however much more easily by applying the Gauss-Bonnet theorem which in our setting says

$$\iint_{\mathcal{S}}K\mathrm{d}\mathcal{A}=\int_0^{2\pi}\int_{-\omega/2}^{\omega/2}K\sqrt{EG-F^2}\mathrm{d}u\mathrm{d}v=4\pi r\int_{-\omega/2}^{\omega/2}\left(\frac{2\wp(u)-r^2}{2\wp(u)+r^2}\right)^3\mathrm{d}u=4\pi$$

and therefore we obtain directly the identity

$$\int_{-\omega/2}^{\omega/2}\left(\frac{2\wp(u)-r^2}{2\wp(u)+r^2}\right)^3\mathrm{d}u=\frac{1}{r}\cdot \tag{29}$$

Replacing this identity back in (28) we produce the final result thereby a simple cancelation!

Regarding the volume of the balloon we have respectively

$$\mathcal{V} = 2\pi\int\limits_0^{\omega/2} x^2 \mathrm{d}z = \pi\int\limits_{-\omega/2}^{\omega/2} x^4(u)\mathrm{d}u = \pi r^4 \int\limits_{-\omega/2}^{\omega/2} \left(\frac{2\wp(u) - r^2}{2\wp(u) + r^2}\right)^4 \mathrm{d}u$$

$$= 2\pi r^4 \left(\frac{\omega}{2} - 4r^2 J_1 + 12 r^4 J_2 - 16 r^6 J_3 + 8 r^8 J_4\right) = \frac{1}{3}\pi\tilde{\omega} r^3.$$

Next in this sequence of integrals is that one of the fifth degree for which we have not an appropriate candidate. However that one of the sixth degree is related to another important mechanical characteristic of the "solid" balloon, namely – its moment of inertia $\mathcal{J}$ about the symmetry axis as it is given by the formula

$$\mathcal{J} = \frac{\pi\rho}{2}\int\limits_{-\omega/2}^{\omega/2} x^4 \mathrm{d}z = \frac{\pi\rho}{2} r^6 \int\limits_{-\omega/2}^{\omega/2} \left(\frac{2\wp(u) - r^2}{2\wp(u) + r^2}\right)^6 \mathrm{d}u$$

$$= \pi\rho r^6 \Big(\frac{\omega}{2} - 6r^2 J_1 + 30 r^4 J_2 - 80 r^6 J_3 + 120 r^8 J_4 - 96 r^{10} J_5 + 32 r^{12} J_6\Big)$$

$$= \frac{3\pi^2 r^5 \rho}{10\tilde{\omega}}.$$

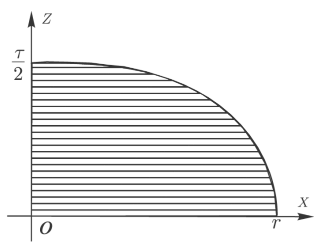

Figure 2. One fourth of the meridional section of the balloon.

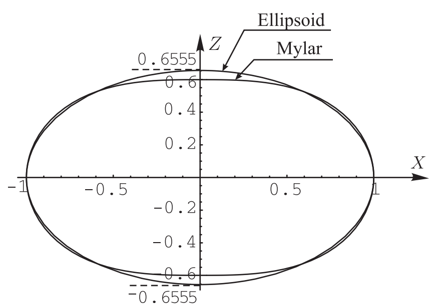

Figure 3. Aspect ratios of the ellipsoid and the mylar balloon with the same radii and volumes.

Here ρ denotes the mass density and one can express $\mathcal{J}$ as functions of $\mathcal{V}$ and the total mass $\mathcal{M} = \mathcal{V}\rho$ of the balloon as follows

$$\mathcal{J} = \frac{9\pi}{10\tilde{\omega}^2}\mathcal{V}\rho r^2 = \frac{9\pi}{10\tilde{\omega}^2}\mathcal{M} r^2. \tag{30}$$

The numerical factor in front of the last expression equals approximately to 0.41127 and has to be compared with that for the axially symmetric ellipsoid with the same mass and equatorial radius which is just 0.4. The aspect ratio of such ellipsoid, i.e., $\eta = c/r$ ($2c$ is the length of the symmetry axis of the ellipsoid) is

$$\eta = \frac{\tilde{\omega}}{4} \approx 0.6555.$$

The profiles of the ellipsoid and the balloon are shown together in Fig. 3.

Another interesting observation is about the area of the deflated balloon (which is $2\pi a^2$ since it consists of two disks of radius a) compared with the area of the inflated one – we find that the ratio of these two areas is larger than one

$$\frac{2\pi a^2}{\pi^2 r^2} = \frac{2}{\pi}\left(\frac{a}{r}\right)^2 = \frac{2}{\pi}\left(\frac{\tilde{\omega}}{2}\right)^2 \approx 1.09422. \tag{31}$$

Following Paulsen [12] this strange result can be easily explained. Our initial model assumption was that Mylar cannot stretch, but this did not mean that it could not shrink. In reality however, the Mylar does not shrink and the shape of the true Mylar balloon differs slightly from the ideal shape above by forming crimping or wrinkling along the sewn equator of the inflated balloon in order to accommodate this $9\,\%$ excess area. While the total redundant area is known, it is interesting to also know its local distribution. For that purpose, following Paulsen, we introduce the so called *crimping factor*, which is defined as the ratio of the surface area of a small patch on the deflated balloon to the corresponding patch on the rectified balloon. The formula derived for this factor in [12] is

$$C(x) = \frac{r^2}{x}\int\limits_0^x \frac{\mathrm{d}t}{\sqrt{r^4 - t^4}}\,, \qquad 0 \le x \le r. \tag{32}$$

In our notation (see (4)) the above elliptic integral reduces to one that is trivial to evaluate

$$C(x) = \tilde{C}(u) = r\frac{2\wp(u) + r^2}{2\wp(u) - r^2}\int\limits_u^{\omega/2} \mathrm{d}\tilde{u} = r\frac{2\wp(u) + r^2}{2\wp(u) - r^2}(\frac{\omega}{2} - u). \tag{33}$$

As it is expected, there is no crimping at the North Pole of the balloon at which

$$C(0) = \lim_{x\to 0} C(x) = \tilde{C}(\frac{\omega}{2}) = \lim_{u\to\frac{\omega}{2}} \tilde{C}(u) = 1 \tag{34}$$

and the maximum crimping occurs at the equator

$$C(r) = \lim_{x\to r} C(x) = \lim_{u\to 0} \tilde{C}(u) = \frac{r\omega}{2}\,\cdot$$

Obviously there is no crimping at the South Pole either.

The expression for the maximum crimping however is nothing else (see (18)) than the ratio of the radii of the deflated and inflated balloon

$$\frac{a}{r} = \frac{\tilde{\omega}}{2} \approx 1.31103. \tag{35}$$

5. Concluding Remarks

In Section 1 of the paper, the mathematical model of the Mylar balloon is presented in the same variational settings, as it was suggested by Paulsen [12]. He had observed that the obtained Euler-Lagrange equation has no closed form solution in terms of elementary functions. By making use of the Gamma function he succeeded to determine three geometrical characteristics – the radius r of the inflated balloon, its thickness τ and the volume $\mathcal{V}$, as being measured versus the radius a of the initially given Mylar disks. In [11], by relying on Maple routines these quantities were obtained numerically.

The first fully analytical depiction of the Mylar balloon has been achieved in [7–9] using elliptic integrals. Here, in Section 2 we give another parametrization of the Mylar balloon via the Weierstrassian functions, and then in Section 3, by exploring with *Mathematica*®, we obtain analytical expressions for the fundamental geometrical characteristics of the balloon. As a result in Section 4 we derive formulas that not only reaffirm the previously obtained expressions, calculated elsewhere via the Gamma function [12] or the elliptic integrals [7–9], but in addition some of them have a more compact form, as it can be seen by a direct comparison of the related expressions.

The constant that plays a key role in the whole description of the Mylar balloon and contributes most for the compactness of the expressions is the lemniscate constant. Historically the lemniscate constant $\tilde{\omega}$ has been discovered as the half-period of the inverse of the lemniscatic integral

$$\int_0^x \frac{\mathrm{d}t}{\sqrt{1-t^4}}$$

and can be defined in relation with the Gauss's constant

$$G = \frac{2}{\pi}\int_0^1 \frac{\mathrm{d}t}{\sqrt{1-t^4}} \approx 0.8346$$

by the equation

$$\tilde{w} = \pi G.$$

References

[1] Abramowitz M. and Stegun I., *Handbook of Mathematical Functions*, Dover, New York 1972.

[2] Djondjorov P., Hadzhilazova M., Mladenov I. and Vassilev V., *Explicit Parameterization of Euler's Elastica*, Geometry, Integrability & Quantization **9** (2008) 175-186.

[3] Ganchev G. and Mihova V., *On the Invariant Theory of Weingarten Surfaces in Euclidean Space*, J. Phys. A: Math. & Theor. **43** (2010) 405210-1-27.

[4] Gibbons G, *The Shape of a Mylar Balloon as an Elastica of Revolution*, DAMTP Preprint, Cambridge University 2006, 7pp.

[5] Greenhill A., *The Applications of Elliptic Functions*, Macmillan, London 1892.

[6] Jahnke E., Emde F. and Losch I., *Tafeln Hoherer Functionen*, Teubner, Stuttgart 1960.

[7] Mladenov I., *On the Geometry of the Mylar Balloon*, C. R. Bulg. Acad. Sci. **54** (2001) 39-44.

[8] Mladenov I. and Oprea J., *The Mylar Balloon Revisited*, Amer. Math. Monthly **110** (2003) 761–784.

[9] Mladenov I., *New Geometrical Applications of the Elliptic Integrals*: *The Mylar Balloon*, J. Nonlinear Math. Phys. Supplement **11** (2004) 55–65.

[10] Oprea J., *Differential Geometry and Its Applications*, 2nd Edn, Prentice Hall, Upper Saddle River 2003.

[11] Oprea J., *The Mathematics of Soap Films*: *Explorations with Maple*, Amer. Math. Society, Providence 2000.

[12] Paulsen E., *What is the Shape of the Mylar Balloon?*, Amer. Math. Monthly **101** (1994) 953–958.

[13] Whittaker E. and Watson G., *A Course of Modern Analysis*, Cambridge University Press, Cambridge 1927.

[14] Wong E. and Guo D., *Special Functions*, World Scientific, Singapore 1989.